

Transition-Metal Nanoparticles

Porphyrin-Stabilized Transition Metal Nanoparticles and Their Applications in the Reduction of 4-Nitrophenol and the Generation of Hydroxyl Radicals

Jiaying Yan,^[a,b] Genjiang Liu,^[a] Ning Li,^[a] Nuonuo Zhang,^[a] and Xiang Liu*^[a]

Abstract: The synthesis of robust transition metal nanoparticles (TMNPs) are still intensively investigated because of multiple up-to date applications in catalysis, solar cells, nonlinear optics, biological labeling, nanoelectronics, medicine and energy storage devices. Here we report synthesis of tetrahydroxyphenylporphyrin (TPP-OH)-stabilized TMNPs (including AuNPs, AgNPs and PdNPs) by mixing TPP-OH and simple commercial metal salt and followed by the addition of sodium borohydride

at 0 °C. The as-synthesized nanocomposites show high catalytic activity in the reduction of 4-nitrophenol, a pertinacious pollutant occurring in industrial waste water. In addition, it is evident that a drastic absorption change has been observed in UV/Vis spectra, confirming that generation of hydroxyl radicals induced by AgNPs and further oxidized methylene blue (MB) to hydroxymethylene blue (MB-OH).

1. Introduction

Transition metal nanoparticles (TMNPs) have gained extensive attention due to their tremendous specific surface area, shape- and size-dependent optical, chemical and physical properties that are totally distinguished from those of the metal blocks.^[1] Therefore, they have been widely used in catalysis, solar cells, nonlinear optics, biological labeling, nanoelectronics, medicines and energy storage devices.^[2] Over the past decades, in order to avoid the agglomeration of TMNPs, many nanoreactors have been designed and developed for stabilizing TMNPs, such as surfactants, dendrimers, cucurbit uril, polymers, biresorcinarenes, cyclodextrins, M₆L₄ capsules, ionic liquids, soft ball, graphene quantum dots and porphyrins.^[3]

Porphyrin and its derivatives are a group of versatile and multifunctional 18 π -electrons conjugated heterocyclic macrocycle organic compounds with fascinating photocatalytic, optical, and chemical properties that have exhibited great potential applications in catalysis,^[4] photodynamic and photothermal therapy,^[5] electrochemical sensor,^[6] antimicrobial material,^[7] cell imaging,^[8] electronic and optical devices through covalent linking to TMNPs.^[9] Porphyrins as stabilizer on transition metal nanoparticles (TMNPs) also have the advantage of exploiting multiple binding sites to obtain a better control of the orientation of porphyrins on the core of TMNPs.^[10] It is still essential

to understand and study effective interaction between porphyrin and TMNPs. Our laboratory has long term interest in the synthesis of porphyrins, their precursors, and their applications.^[11] Hence, in the present study, we first report tetrahydroxyphenylporphyrin (TPP-OH)-stabilized Au-, Ag- and PdNPs and their applications in the reduction of 4-nitrophenol and production of hydroxyl radicals. The four hydroxy groups present in the periphery of the porphyrin has a decisive effect on stabilizing the nanoparticles in a controlled fashion to prevent the aggregation. Construction of the TMNPs has been conducted by here direct coordination of transition metal ions onto stoichiometric porphyrin followed by NaBH₄ reduction in the mixture of ethanol and water. Then Au-, Ag- and PdNPs's compared catalytic performance in 4-nitrophenol reduction by NaBH₄ has been scrutinized by kinetic studies including induction times and determinations of rate constants in water. In addition, AgNPs has also been measured for the induced the accumulation of hydroxyl radicals in the presence of hydrogen peroxide.

2. Results and Discussion

2.1. Synthesis of the Porphyrin-Stabilized TMNPs

First, tetrahydroxyphenylporphyrin (TPP-OH) is known and has been easily assembled by classical cyclocondensation of *p*-hydroxybenzaldehyde and pyrrole in the presence of propionic acid in dimethyl sulfoxide at 140 °C for 2 h.^[12] The synthesis of TPP-OH-stabilized AuNPs **1–3** was conducted by using as synthesized TPP-OH and simple commercial chloroauric acid dissolved in the mixture of EtOH (1 mL) and water (9 mL) in a standard molar ratio 2:1, 1:1 or 1:2 of metal ion/porphyrin and followed by the addition of sodium borohydride as the reductant at 0 °C,

[a] College of Materials and Chemical Engineering, Key Laboratory of Inorganic Nonmetallic Crystalline and Energy Conversion Materials, China Three Gorges University, Yichang, Hubei 443002, China
E-mail: xiang.liu@ctgu.edu.cn

[b] State Key Laboratory of Coordination Chemistry, Nanjing University, Nanjing, Jiangsu, 210093, P.R. China

Supporting information and ORCID(s) from the author(s) for this article are available on the WWW under <https://doi.org/10.1002/ejic.201900172>.

respectively (Figure 1). EtOH has been added for dissolving porphyrin, Au^{III} ions were bonded to a nitrogen or oxygen atom of the porphyrin, and the corresponding nanoparticles had a small size and were good catalysts. These porphyrin ligands are neutral and weak, leaving the surface atoms in a zero oxidation state by the reduction of sodium borohydride. However, the characteristic peaks of AuNPs did not appear in the UV/Vis spectra, due to the interference of porphyrins. In addition, the stability of **AuNPs-2** has also been investigated, AuNPs solution is stirred for 2 h at 45 °C, 60 °C, 75 °C and 90 °C, respectively. We found **AuNPs-2** is very stable even at 90 °C for 2 h (Figure S11–S14 in the Supporting Information). Then TEM have been measured to further confirm the morphology and size of the AuNPs. As shown in Figure 2a–2c, we found the sizes of **AuNP-2** (3.2 nm) is much smaller than those of **AuNP-1** (3.8 nm) and **AuNP-3** (4.8 nm). The size of these AuNPs also is modulated by variation of the volume ratio of ethanol in the solution, then the **AuNP-4** (4.1 nm) and **AuNP-5** (4.0 nm) are obtained in the mixture of EtOH (2 mL)/water (8 mL) and EtOH (4 mL)/water (6 mL) as the same condition as **AuNP-2**, respectively (Figure 2d and Figure 2e). Moreover, the size of these AuNPs is also modulated by variation of the reaction temperature. **AuNP-6** (5.5 nm), obtained at 30 °C (Figure 2f), is much larger than **AuNP-2** at 0 °C (3.2 nm). It is probably on account of Ostwald ripening that occurs at 30 °C following Au atom nucleation, however, resulting in the decrease in the number of Au nuclei and to AuNPs overgrowth. Thus, the standard molar ratio 1:1 of metal ion/porphyrin, 0 °C and volume ratio 1:9 of EtOH/water are the optimal conditions. Therefore, PdNPs and AgNPs have been synthesized as the same condition as **AuNP-2**. The TEM image shows the size of PdNPs is only 1.7 nm, while AgNPs (14 nm) is much larger (Figure 3). To further verify the formation of TMNPs, the X-ray photoelectron spectroscopy (XPS) spectra of **AuNP-2**

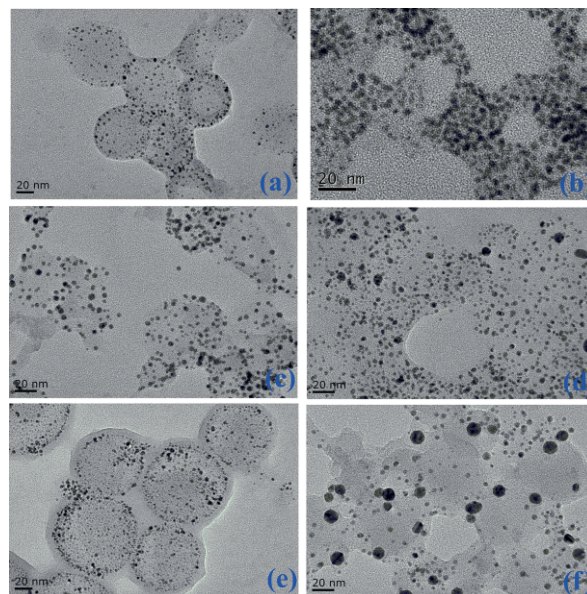


Figure 2. TEM images of AuNPs. (a)–(f): 1–6.

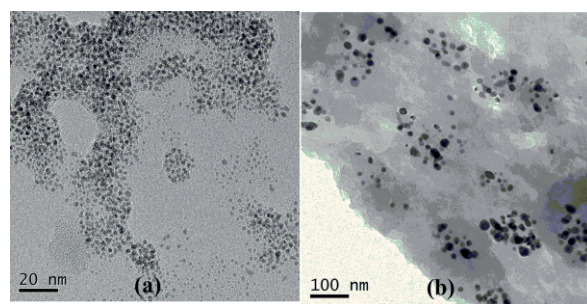


Figure 3. (a) TEM image of PdNPs. (b) TEM image of AgNPs.

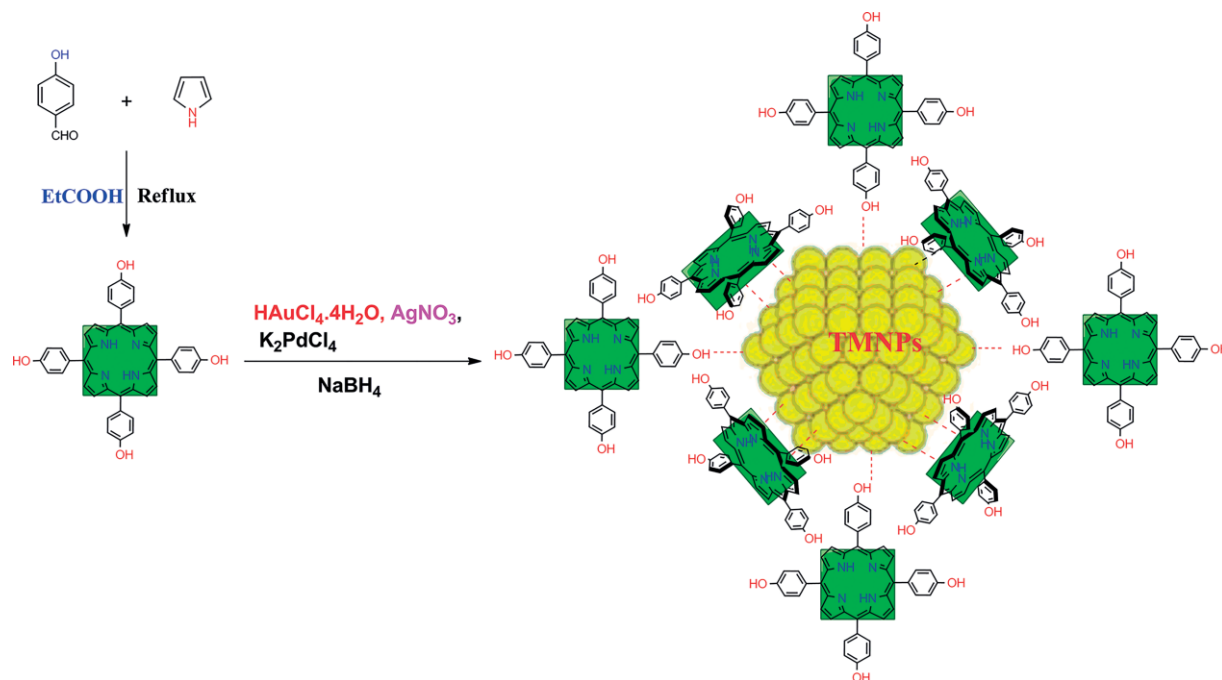


Figure 1. Schematic illustration of the synthesis of TPP-OH-stabilized Au-, Ag-, and PdNPs.

and AgNPs have been measured. **AuNP-2** only exhibits Au⁰ on the surface atoms of AuNP in the XPS, Au 4f peaks positions at 83.0 and 87.0 eV. The binding energy of 83.0 eV and 87.0 eV for Au 4f_{7/2} and 4f_{5/2}, respectively (Figure 4a). Similarly, XPS of AgNPs exhibits Ag 3d peaks positions at 368.1 eV and 374.0 eV. The binding energy of 368.1 eV and 374.0 eV for Ag 3d_{5/2} and 3d_{3/2}, respectively, are exclusively assigned to the zero-valent surface atoms of AgNPs (Figure 4b), more discussion has been provided in the Supporting Information.

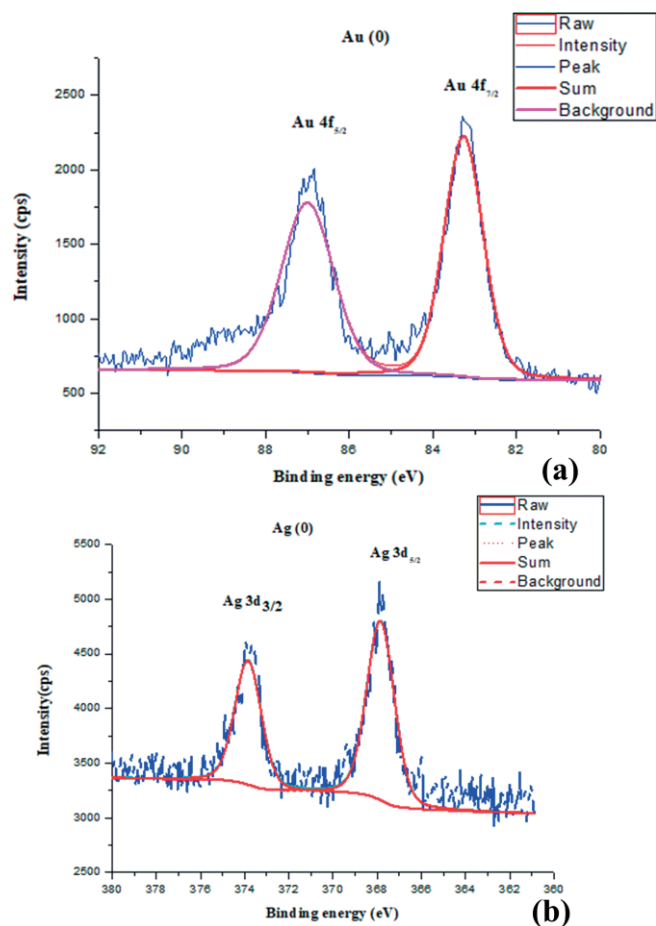
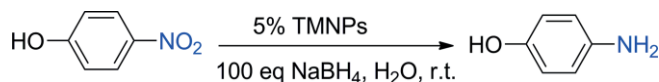


Figure 4. (a) XPS of AuNP-2, (b) XPS of AgNPs.

Table 1. 4-Nitrophenol reduction catalyzed by TMNPs in water.^[a]



Entry	TM ions [mmol]	EtOH [mL]	TMNPs	T ₀ [s] ^[c]	K _{app} ^[d] [× 10 ⁻³ s ⁻¹]	D [nm] ^[e]
1	1.25×10 ⁻⁴	1	AuNP-1	300	3.7	3.8
2	2.5×10 ⁻⁴	1	AuNP-2	180	8	3.2
3	5.0×10 ⁻⁴	1	AuNP-3	180	3.3	4.8
4	2.5×10 ⁻⁴	2	AuNP-4	180	1.4	4.1
5	2.5×10 ⁻⁴	4	AuNP-5	300	0.4	4.0
6 ^[b]	2.5×10 ⁻⁴	1	AuNP-6	420	2.9	5.5
7	2.5×10 ⁻⁴	1	PdNPs	0	4	1.7
8	2.5×10 ⁻⁴	1	AgNPs	–	–	14.0

[a] 5.0 mol-% AuNPs@GQDs were used in the catalyzed 4-nitrophenol reduction NaBH₄ is in excess (100:1). All the AuNPs 1–5 were synthesized at 0 °C except 6. [b] AuNPs@GQDs 6 were synthesized at 30 °C. [c] Induction time. [d] Rate constant. [e] Core size (TEM) of the TMNPs.

2.2. Comparing Catalytic Activities of TMNPs in 4-Nitrophenol Reduction

4-Nitrophenol, a common by-product in industry, is regarded as one class of the most highly hazardous and toxic pollutants.^[13] It has a delayed interaction with blood and forms methaemoglobin which is responsible for methemoglobinemia, potentially causing confusion, cyanosis, and unconsciousness. The catalytic reduction of 4-nitrophenol by sodium borohydride in water was chosen as a model reaction to evaluate the catalytic efficiency of TMNPs (Table 1 and Fig. S17–S30 in the Supporting Information). The reduction of 4-nitrophenol has been carried out in the presence of 5.0 mol-% TMNPs with 100 equiv. of NaBH₄ in water at room temperature, this large excess NaBH₄ being usually utilized to induce an obvious first-order kinetics and a relative lack of competitive NaBH₄ hydrolysis by water as solvent. Based on the experimental result, all reactions need an induction time of 180s to 420s in the presence of these AuNPs 1–6, related to the reorganization at the catalyst surface (Table 1, entries 1–6). This induction time is taken into account by the stabilization of the AuNPs with porphyrin that the steric bulk inhibiting substrate approach to the AuNPs surface as a consequence of intradendritic porphyrin of AuNPs. Among them, the reaction rate *k*_{app} of **AuNP-2** (8 × 10⁻³) is much higher than these of **AuNP-1** (3.7 × 10⁻³) and **AuNP-3** (3.3 × 10⁻³). The reaction rate *k*_{app} of AuNP-4 and 5 decreases with as the increase of amount of EtOH in the process of the synthesis (Table 1, entries 4 and 5). It is clear that AuNP-2 shows the highest reaction rate among these AuNPs (Table 1, entry 6), this is consistent with the smallest size of 3.2 nm. Catalysis by PtNPs was found not to need an induction time (Table 1, entry 7), while AgNPs is inactive (Table 1, entry 8). Thus, the reaction rate *k*_{app} increases in the order Ag < Pd < Au. In addition, TPP-OH alone do not catalyze the degradation of 4-nitrophenol under these conditions (the yellow color of 4-nitrophenol does not change to colorless in two weeks).

2.3. Effect of AgNPs on ·OH Generation

It is well-known that the Fenton-like reaction between AgNPs and H₂O₂, which could generate powerful oxidizing species

such as $\cdot\text{OH}$.^[14] The oxidized and reduced forms of methylene blue (MB) have different absorption bands in the UV/Vis spectrum. Hence, the progress of $\cdot\text{OH}$ oxidized reaction from MB to MB-OH can be monitored by measuring the decrease in absorption of MB on UV/Vis spectrum at a peak of 666 nm (Figure 5).^[15] The time dependent UV/Vis spectrum of MB during 0.025 mmol/L AgNPs and 0.125 mmol/L (5 equiv.) H_2O_2 is presented in Figure 6a. After 20 min, MB peak intensity decreases 0.085. As expected, it is evident that a drastic absorption

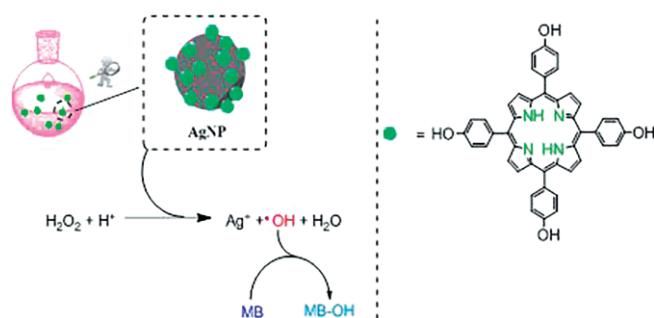


Figure 5. Schematic illustration of $\cdot\text{OH}$ generation by AgNPs.

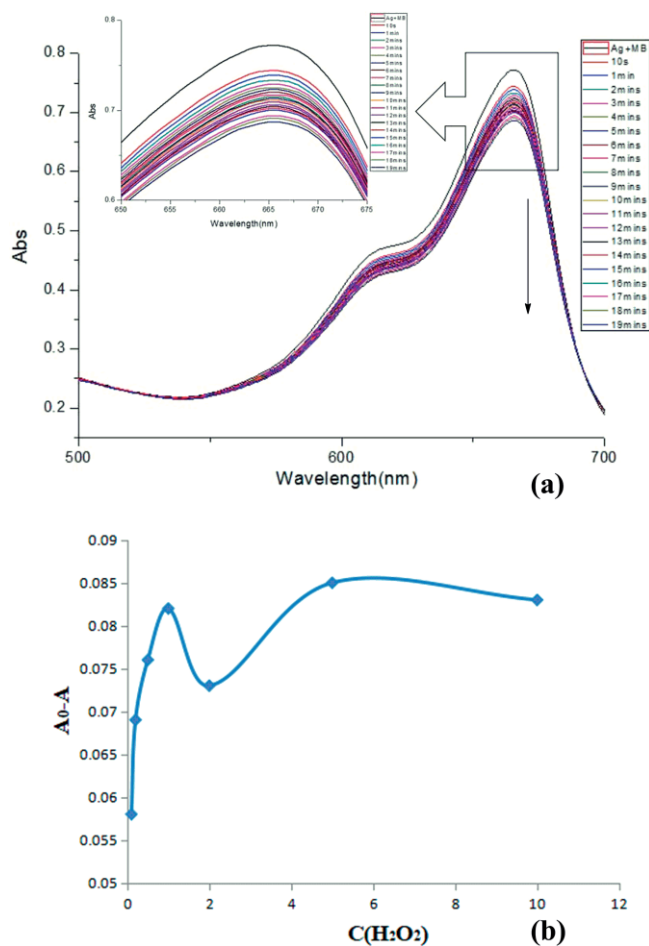


Figure 6. (a) UV/Vis absorption spectra for the oxidation of methylene blue by AgNPs and 5 eq H_2O_2 . (b) Effect of H_2O_2 on the generation of hydroxyl radicals from samples containing 3 mL of 0.25 mmol/L AgNPs, 9 μL of 2.5 mmol/L methylene blue and H_2O_2 at different concentrations.

change could be observed, confirming that generation of hydroxyl radicals induced by AgNPs and further oxidized MB to MB-OH. Then the influence of hydrogen peroxide concentration on the generation of hydroxyl radicals has been studied as shown in Figure 6b (Figure S31–S36 in the Supporting Information). The production of hydroxyl radicals was quasi-linearly proportional to the concentration of H_2O_2 from 0.1 eq to 1.0 eq, compared to the amount of AgNPs. At the amount of H_2O_2 above 1 eq, generation of hydroxyl radicals no longer increased indicating a saturation of the reactivity of AgNPs. When added without AgNPs or H_2O_2 , MB peak intensity remains unchanged. This is totally consistent with the proposed Fenton-like reaction between AgNPs and hydrogen peroxide to generate hydroxyl radicals.

3. Conclusion

A green and facile method of synthesis of tetrahydroxyphenylporphyrin (TPP-OH)-stabilized TMNPs has been developed in this work. Construction of AuNPs 1–6, AgNPs and PdNPs nanocomposites is accomplished by mixing TPP-OH and simple commercial metal salt followed by the addition of sodium borohydride at 0 °C. TEM images show that the sizes of AuNP-2 and AgNP are 3.2 nm and 14.0 nm, respectively. Then Au-, Ag- and PdNPs's compared catalytic performance in 4-nitrophenol reduction by NaBH_4 has been scrutinized by kinetic studies including induction times and determinations of rate constants in water. In addition, AgNPs has also been measured for the induced the accumulation of hydroxyl radicals in the presence of hydrogen peroxide. As expected, it is evident that a drastic absorption change has been observed in UV/Vis spectra, confirming that generation of hydroxyl radicals induced by AgNPs and further oxidized MB to MB-OH. Therefore, we expect that these TMNPs nanocomposites may offer wide potential applications in sensors, clinical diagnosis and catalysis fields.

Experimental Section

1. Preparation of Tetrahydroxyphenylporphyrin (TPP-OH): TPP-OH has been synthesized following reference 12 of the main text. First, 60 mL of EtCOOH and 3 mL of DMSO have been put into 250 mL round-bottom flask, it is then heated to reflux. *p*-hydroxybenzaldehyde (3 g, dissolved in 10 mL of EtCOOH) and pyrrole (0.0025 mol, dissolved in 10 mL of EtCOOH) have been added to flask. The reaction mixture is stirred for 2 h under reflux. After cooling to room temperature, EtCOOH was removed under vacuum in which EtOH (≈ 30 mL) was added. Under 0 °C, the desired TPP-OH as a deep green solid was obtained after filtration. ^1H NMR (300 MHz, CDCl_3): δ = 9.92 (s, 4H), 8.81 (s, 8H), 7.94–7.95 (d, 8H), 7.14–7.16 (d, 8H), –2.95 (s, 2H). ESI HRMS: calcd. for $\text{C}_{44}\text{H}_{30}\text{N}_4\text{O}_4$ [$\text{M} + \text{H}$] $^+$: 679.2267, found 679.2332.

2. Preparation of the TPP-OH Stabilized Transition Metal Nanoparticles: First, 2.5×10^{-4} mmol TPP-OH is dissolved in 1 mL of EtOH in a Schlenk flask with 7 mL of deionized water, and the solution is stirred for 10 min at 0 °C. And a colorless solution of $\text{HAuCl}_4 \cdot 3\text{H}_2\text{O}$ (2.5×10^{-4} mmol in 1.0 mL of water) is added to the solution of TPP-OH. And the solution is stirred for 30 min. A 1-mL aqueous solution containing 2.5×10^{-3} mmol of NaBH_4 is added

dropwise, provoking the formation of purple (AuNP) color corresponding to the reduction of the cation to the zero-valent metal and AuNP-2 formation. The AuNP-2 were kept in aqueous solution for characterization and used as the catalysts. Other TMNPs were synthesized using the same method.

3. Catalysis of 4-Nitrophenol Reduction: An aqueous solution (2.5 mL) containing 4-nitrophenol (0.09 mmol) and NaBH₄ (9 mmol) is prepared in a standard quartz cuvette (3 mL, path length: 1 cm). The TMNPs catalyst (5 mol-%) is injected into this solution, and the reaction progress is detected by UV/Vis. spectroscopic analysis every min at 22 °C. (Figure S17–S30).

4. Generation of Hydroxyl Radicals: An aqueous solution containing 3 mL of AgNPs (0.025 mmol/L) and 9 μL methylene blue (2.5 mmol/L) is prepared in a standard quartz cuvette (3 mL, path length: 1 cm). The H₂O₂ (0.1 eq –10 equiv.) is injected into this solution, and the reaction progress is detected by UV/Vis. spectroscopic analysis every min at 22 °C. (Figure S31–S36).

Acknowledgments

Financial support from the National Natural Science Foundation of China (Grant Nos. 21805166 and 21606145), the 111 Project of Hubei Province (Grant No. 2018-19-1), the State Key Laboratory of Coordination Chemistry Foundation of Nanjing University (No. SKLCC1811), and China Three Gorges University is gratefully acknowledged.

Keywords: Porphyrin · Nanoparticles · 4-Nitrophenol · Reduction · Radicals

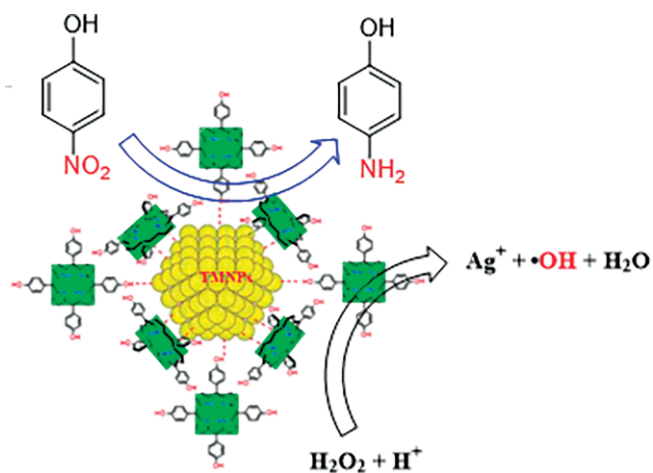
- [1] a) M. Sankar, N. Dimitratos, P. J. Miedziak, P. P. Wells, C. J. Kiely, G. J. Hutchings, *Chem. Soc. Rev.* **2012**, *41*, 8099; b) X. Liu, D. Astruc, *Adv. Mater.* **2017**, *29*, 1605305; c) Y. Zhu, N. S. Hosmane, *Coord. Chem. Rev.* **2015**, *293*, 357; d) M.-C. Daniel, D. Astruc, *Chem. Rev.* **2004**, *104*, 293; e) X. Liu, C. Manzur, N. Novoa, S. Celedon, D. Carrillo, J.-R. Hamon, *Coord. Chem. Rev.* **2018**, *357*, 144–172; f) S. Cao, F. Tao, Y. Tang, Y. Li, J. Yu, *Chem. Soc. Rev.* **2016**, *45*, 4747–4765.
- [2] a) L. Liu, A. Corma, *Chem. Rev.* **2018**, *118*, 4981–5079; b) X. Liu, D. Astruc, *Adv. Synth. Catal.* **2018**, *360*, 3426–3459; c) H. Kang, J. T. Buchman, R. S. Rodriguez, H. L. Ring, J. He, K. C. Bantz, C. L. Haynes, *Chem. Rev.* **2019**, *119*, 664–699; d) X. Liu, D. Astruc, *Coord. Chem. Rev.* **2018**, *359*, 112–126; e) J. J. Soldevila-Barreda, N. Metzler-Nolte, *Chem. Rev.* **2019**, *119*, 829–869.
- [3] a) V. Chechik, R. M. Crooks, *J. Am. Chem. Soc.* **2000**, *122*, 1243; b) D. Wang, D. Astruc, *Chem. Soc. Rev.* **2017**, *46*, 816–854.
- [4] a) K. S. Lokesh, A. Shambhulinga, N. Manjunatha, M. Imadadulla, M. Hojamberdiev, *Dyes Pigm.* **2015**, *120*, 155–160; b) P. Mineo, A. Abbadessa, A. Mazzaglia, A. Gulino, V. Villari, N. Micali, S. Millesi, C. Satriano, E. Scamporrino, *Dyes Pigm.* **2017**, *141*, 225–234; c) I. Fratoddi, C. Battocchio, G. Polzonetti, F. Scuibba, M. Delfini, M. V. Russo, *Eur. J. Inorg. Chem.* **2011**, 4906–4913.
- [5] a) M. E. Alea-Reyes, J. Soriano, I. Mora-Espí, M. Rodrigues, D. A. Russell, L. Barrios, L. Pérez-García, *Colloids Surf. B* **2017**, *158*, 602–609; b) J. Zeng, W. Yang, D. Shi, X. Li, H. Zhang, M. Chen, *ACS BioMater. Sci. Eng.* **2018**, *4*, 963–972; c) O. J. Fakayode, S. P. Songca, O. S. Oluwafemi, *Mater. Lett.* **2017**, *199*, 37–40.
- [6] B. Kaur, K. Malecka, D. A. Cristaldi, C. S. Chay, I. Mames, H. Radecka, J. Radecki, E. Stulz, *Chem. Commun.* **2018**, *54*, 11108–11111.
- [7] O. Lyutakov, O. Hejna, A. Solov'yev, Y. Kalachyova, V. Svorcik, *RSC Adv.* **2014**, *4*, 50624–50630.
- [8] N. C. M. Tam, P. Z. McVeigh, T. D. MacDonald, A. Farhadi, B. C. Wilson, G. Zheng, *Bioconjugate Chem.* **2012**, *23*, 1726–1730.
- [9] M. Drobizhev, Y. Stepanenko, A. Rebane, C. J. Wilson, T. E. O. Screen, H. L. Anderson, *J. Am. Chem. Soc.* **2006**, *128*, 12432–12433.
- [10] T. Hasobe, *Phys. Chem. Chem. Phys.* **2010**, *12*, 44–57.
- [11] a) J. Yan, Y. Yang, M. Ishida, S. Mori, B. Zhang, Y. Feng, H. Furuta, *Chem. Eur. J.* **2017**, *23*, 11375–11384; b) N. Zhang, J. Chen, K. Cheng, Y. Li, L. Wang, K. Zheng, Q. Yang, D. Li, J. Yan, *Res. Chem. Intermed.* **2017**, *43*, 2921; c) Y. Li, J. Yan, K. Cheng, S. Kong, K. Zhang, L. Wang, N. Zhang, *Res. Chem. Intermed.* **2017**, *43*, 5337; d) J. Yan, M. Takakusaki, Y. Yang, S. Mori, B. Zhang, Y. Feng, M. Ishida, H. Furuta, *Chem. Commun.* **2014**, *50*, 14593–14596; e) N. Zhang, B. Zhang, J. Yan, X. Xue, X. Peng, Y. Li, Y. Yang, C. Ju, C. Fang, Y. Feng, *Renewable Energy* **2015**, *77*, 579–585; f) Y. J. Li, J. Yan, S. Xiao, B. Zhang, F. Lu, K. Cheng, D. Li, Y. Feng, N. N. Zhang, *Tetrahedron Lett.* **2016**, *57*, 3226–3230; g) X. Liu, J.-R. Hamon, *Coord. Chem. Rev.* **2019**, *389*, 94–118; h) T. T. Zhang, Y. J. Li, J. Yan, Y. Liang, B. B. Xu, K. B. Zheng, N. N. Zhang, *Tetrahedron* **2018**, *74*, 2807–2811; i) Y. Zhou, J. Yan, N. Zhang, D. Li, S. Xiao, K. Zheng, *Sensor Actuat. B-Chem.* **2018**, *258*, 156–162; j) M. Li, K. Zheng, H. Chen, X. Liu, S. Xiao, J. Yan, X. Tan, N. Zhang, *Spectrochim. Acta Part A* **2019**, *217*, 1–7.
- [12] Z. Hou, W. Dehaen, J. Lyskawa, P. Woisel, R. Hoogenboom, *Chem. Commun.* **2017**, *53*, 8423–8426.
- [13] P. Zhao, X. Feng, D. Huang, G. Yang, D. Astruc, *Coord. Chem. Rev.* **2015**, *287*, 114–136.
- [14] a) L. Wang, J. Zheng, Y. Li, S. Yang, C. Liu, Y. Xiao, J. Li, Z. Cao, R. Yang, *Anal. Chem.* **2014**, *86*, 12348–12354; b) L.-Y. Duan, Y.-J. Wang, J.-W. Liu, Y.-M. Wang, N. Li, J.-H. Jiang, *Chem. Commun.* **2018**, *54*, 8214–8217; c) H. Jiang, Z. Chen, H. Cao, Y. Huang, *Analyst* **2012**, *137*, 5560–5564.
- [15] S. Naraginti, F. B. Stephen, A. Radhakrishnan, A. Sivakumar, *Spectrochim. Acta A* **2015**, *135*, 814–819.

Received: February 14, 2019

Transition-Metal Nanoparticles

J. Yan, G. Liu, N. Li, N. Zhang,
X. Liu* 1–6

 **Porphyrin-Stabilized Transition Metal Nanoparticles and Their Applications in the Reduction of 4-Nitrophenol and the Generation of Hydroxyl Radicals**



Here we report the synthesis of tetrahydroxyphenylporphyrin-stabilized TMNPs by mixing TPP-OH and simple commercial metal salt followed by the addition of sodium borohydride. The

as-synthesized nanocomposites show high catalytic activity in the reduction of 4-nitrophenol and the generation of hydroxyl radicals.

DOI: 10.1002/ejic.201900172